Using Lie algebra for shape estimation of medical snake robots

Rangaprasad Arun Srivatsan, Matthew Travers and Howie Choset

***Abstract*— Highly articulated robots have the potential to play a key role in minimally invasive surgeries by providing improved access to hard-to-reach anatomy. Estimating their shape inside the body and combining it with 3D preoperative scans of the anatomy enable the surgeon to visualize how the entire robot interacts with the internal organs. As the robot progresses inside the body, the position and orientation of every link comprising the robot, evolves over a coordinate-free Lie algebra, $se(3)$. To capture the full motion and uncertainty of the system, we use an extended Kalman filter where the state vector is defined using elements of $se(3)$. We show that this approach describes the shape of the robot more accurately, than the ones where the state vector is a conventional parametrization, such as Cartesian coordinates and Euler angles. We perform two experiments to demonstrate the effectiveness of this new filtering approach.**

I. INTRODUCTION

When compared to conventional procedures, minimally invasive surgeries (MIS) have potential benefits including "reduced-pain", minimal "blood-loss", faster healing and reduced tissue disruption. To further improve upon MIS, our group, along with others [1]–[4] have been developing snake-like robots to provide deeper access to the anatomy with fewer incisions. However, robot-guided MIS introduces other drawbacks like lack of situational awareness and limited sensory feedback. This forces surgeons to use their expertise in finding relation between pre-operative images and the surgical reality. Although emerging technologies like fiber optics, MRI, ultrasound and CT have proved to be useful, they suffer from limited field of view and incompatibility with robot systems.

Prior efforts include generating 3D models of anatomical structures from pre-operative scans and combining them with model-based tool tracking, to create a virtual view of the operation for visual feedback. To successfully use this technique, the tool needs to be registered in the frame of reference of the 3D model. A number of algorithms have been developed to take input from electro-magnetic sensors [5], ultrasound [6], [7] etc., and help in the registration process.

When the tool is a highly articulated robot, estimation is more difficult because of the additional degrees of freedom (DOFs). Also complete knowledge of its shape configuration is necessary to avoid interfering with organs. In [8] a nonlinear stochastic filtering method is used to estimate the shape and configuration of a snake robot (see Fig. 1). It measures the pose of the tip and prescribes a motion model based on the robot's kinematics and history of the previous inputs. The state of the snake robot, both its base pose and its internal shape, is described in terms of Cartesian coordinates and Euler angles. In presence of high uncertainties, this parametrization does a poor job of estimating the shape of the robot. However, recent work by Long et al [9] shows that modeling a system using exponential coordinates yields better estimation as opposed to using conventional parameters especially in the presence of large uncertainties.

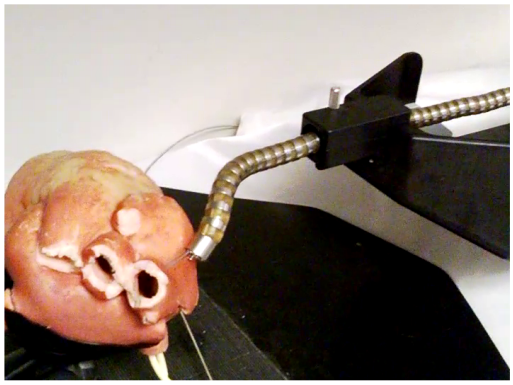

Fig. 1. The high DOF snake robot used in this work

Exploiting the underlying structure of the Lie group and algebra which defines motions for the robot, in this work we use an extended Kalman filter (EKF) framework to estimate the state of the system that is described by exponential coordinates. This approach provides better estimate of shape than using a conventional parametrization [10]. In general it is not trivial to obtain closed-form expressions for the filter's process and measurement models in terms of exponential coordinates as opposed to other parametrizations of $SE(3)$; and hence prior work use Cartesian coordinates in combination with quaternions, Euler angles or Rodrigues parameters [11]. An important contribution of this paper is deriving closed form analytical expressions for the motion model to estimate the state of the robot defined in terms of exponential coordinates.

The rest of the paper is organized as follows: In Section 2, the motivation for this work is explained in detail. The description of elements of the state vector used in the EKF is provided in Section 3. Section 4 discusses the motion model and measurement model required for the EKF. In Section 5, experimental results are provided and finally conclusions are discussed in Section 6.

[1]R. Arun Srivatsan, M. Travers and H. Choset are with the Robotics Institute at Carnegie Mellon University, Pittsburgh, PA 15213, USA, arangapr@andrew, mtravers@andrew, choset@cs.cmu.edu

II. Motivation

We start our discussion of by first estimating the position and orientation of a rigid body, which is typically described by a $\boldsymbol{g} \in SE(3)$. The special Euclidean group $SE(3)$, is homeomorphic to $\mathbb{R}^3 \times SO(3)$. The elements of $SE(3)$ can be represented by $\boldsymbol{R} \in SO(3)$ and $\boldsymbol{t} \in \mathbb{R}^3$ in the form of the following 4×4 matrix,

$$\boldsymbol{T} = \begin{pmatrix} \boldsymbol{R} & \boldsymbol{t} \\ \boldsymbol{0}_{1\times 3} & 1 \end{pmatrix} \in SE(3). \tag{1}$$

For a vector $\boldsymbol{x} = [v_1, v_2, v_3, \omega_1, \omega_2, \omega_3]^T \in \mathbb{R}^6$, an element $\hat{\boldsymbol{x}}$, of the Lie algebra $se(3)$ can be expressed as,

$$\hat{\boldsymbol{x}} = \begin{pmatrix} \boldsymbol{\Omega} & \boldsymbol{v} \\ \boldsymbol{0}_{1\times 3} & 0 \end{pmatrix} \in se(3), \tag{2}$$

where $\boldsymbol{v} = [v_1, v_2, v_3]^T$ and $\boldsymbol{\Omega}$ is the skew-symmetric matrix formed from $[\omega_1, \omega_2, \omega_3]^T$:

$$\boldsymbol{\Omega} = \begin{pmatrix} 0 & -\omega_3 & \omega_2 \\ \omega_3 & 0 & -\omega_1 \\ -\omega_2 & \omega_1 & 0 \end{pmatrix}. \tag{3}$$

The vector $\boldsymbol{x}$ is referred to as the twist vector and the operator $\hat{}$ is used to map from $\mathbb{R}^6$ to $se(3)$. The twist vector parametrizes an element of the Lie algebra $se(3)$ that belongs to the Lie group $SE(3)$. The element $\boldsymbol{T} \in SE(3)$, corresponding to $\hat{\boldsymbol{x}}$ can be obtained by using a matrix exponential,

$$\boldsymbol{T} = \exp(\hat{\boldsymbol{x}}), \tag{4}$$

and so the twist vector $\boldsymbol{x}$ is also referred to as exponential coordinates.

The $SE(3)$ element can also be obtained using parameters such as Cartesian coordinates that parametrize $\boldsymbol{t}$ and Euler angles that parametrize $\boldsymbol{R}$. However using the Lie algebra gives a coordinate-free way to represent the $SE(3)$ element and hence provides more accurate estimation as shown in [12]. For example, Fig 2 shows the distribution over the Cartesian coordinates for a differentially driven robot moving along a straight line. Note how the probability density function (PDF) contours of Gaussian of best fit are not a good approximate to the distribution. On the other hand, representing the state vector in terms of exponential coordinates, captures the distribution better. Fig 3(a) shows how the PDF contours of Gaussian of best fit in exponential coordinates, approximates the distribution closely. When mapped back into the Cartesian space through the exponential map, the Gaussian contours appear to bend and take a banana-like shape as shown in Fig. 3(b), and approximate the distribution closely.

Exploiting the underlying structure of the Lie group and algebra that defines motions for the robot, we will now use exponential coordinates to define the state of every link of the snake-robot.

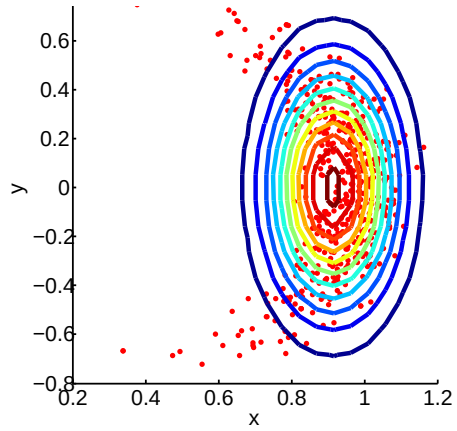

Fig. 2. The PDF contours of Gaussian of best fit in Cartesian coordinates

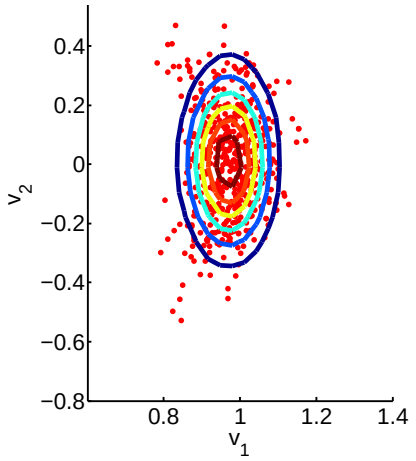

(a) The PDF contours of Gaussian of best fit in exponential coordinates

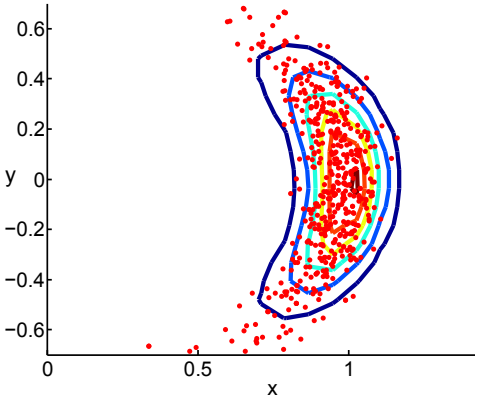

(b) The PDF contours of Gaussian of best fit in exponential coordinates mapped into Cartesian space

Fig. 3. The PDF contours of Gaussian in exponential coordinates and when mapped into Cartesian space

III. Definition of state vector

The state vector for an N link snake robot [13] is described in [8] as $[\boldsymbol{p}_0, \boldsymbol{e}_0, \phi_1, \theta_1, \ldots, \phi_{N-1}, \theta_{N-1}]^T$, where $\boldsymbol{p}_0 = [x_0, y_0, z_0]^T$ and $\boldsymbol{e}_0 = [\alpha_0, \beta_0, \gamma_0]^T$ define the position and orientation respectively of the most proximal link, while ϕ_i, θ_i give the rotation between successive links. In this work, the state vector is formulated in terms of exponential coordinates as,

$$\boldsymbol{x}_k = [\underbrace{v_1^0, v_2^0, v_3^0}_{\boldsymbol{v}}, \underbrace{\omega_1^0, \omega_2^0, \omega_3^0}_{\boldsymbol{\omega_0}}, \omega_2^1, \omega_3^1, \ldots, \omega_2^{N-1}, \omega_3^{N-1}]^T, \tag{5}$$

where $(\boldsymbol{v}^T, \boldsymbol{\omega_0}^T)^T$ is the twist vector that is used to identify the element $\boldsymbol{T}_0 \in SE(3)$ of the most proximal link of the robot. The variables ω_2^i, ω_3^i for each link i are exponential coordinates, representative of the relative rotation between successive links with the subscripts indicating the axis along which they are defined.

A. Filter state

This section establishes the relation between the state vector in [8] and the one in Eq. (5). In doing so we define the notion of state for both the proximal and the remaining links.

1) Proximal link: Given the state vector of the proximal link, $[x_0, y_0, z_0, \alpha_0, \beta_0, \gamma_0]^T$, the rotation matrix is first obtained as $\boldsymbol{R} = \boldsymbol{R_z}(\alpha_0)\boldsymbol{R_y}(\beta_0)\boldsymbol{R_x}(\gamma_0)$, where $\boldsymbol{R_k}(\phi)$ is the rotation matrix describing the rotation about axis $\boldsymbol{k}$ by an angle ϕ. Upon obtaining $\boldsymbol{R}$, the matrix logarithm of $\boldsymbol{R}$ is evaluated to obtain the angular velocity $\boldsymbol{\omega^0} = [\omega_1^0, \omega_2^0, \omega_3^0]^T$ as shown in [14]. We obtain the following:

$$\widehat{\boldsymbol{\omega^0}} = \frac{\theta}{2\sin\theta}(\boldsymbol{R} - \boldsymbol{R}^T), \tag{6}$$

where $\theta = \arccos\left(\frac{\text{trace}(\boldsymbol{R})-1}{2}\right)$ and $\boldsymbol{R} \neq \boldsymbol{I}_{3\times3}$. Note that, if $\boldsymbol{R} = \boldsymbol{I}_{3\times3}$, then $\theta = 2\pi k$, where k is any integer and $\boldsymbol{\omega^0}$ can be chosen arbitrarily. Having obtained $\boldsymbol{\omega}^0$, the linear velocity $\boldsymbol{v} = [v_1, v_2, v_3]^T$ can obtained as follows:

$$\boldsymbol{v} = \boldsymbol{W}[x_0, y_0, z_0]^T, \tag{7}$$

where $\boldsymbol{W} = \boldsymbol{I}_{3\times3} - \frac{\widehat{\boldsymbol{\omega^0}}}{2} + \left(1 - \frac{\theta\sin\theta}{2(1-\cos\theta)}\right)\frac{\widehat{\boldsymbol{\omega^0}}^2}{\theta^2}$. Note that if $\theta = 0$, then $\boldsymbol{W} = \boldsymbol{I}_{3\times3}$.

2) Distal links: The relative rotation between successive links is represented by ϕ_i and θ_i in [8]. Let the exponential coordinates describing the relative motion between successive links be $[v_1^i, v_2^i, v_3^i, \omega_1^i, \omega_2^i, \omega_3^i]^T$. The equivalent of this in the exponential coordinates can be obtained by following the procedure used in the case of the proximal link. The relative motion between links is purely rotational and so we have, $v_1^i = 0, v_2^i = 0, v_3^i = 0$. Further since there is no roll motion between successive links, $\omega_1^i = 0$. Thus ω_2^i, ω_3^i alone are sufficient to describe the relative motion. Taking advantage of the way ϕ_i, θ_i are defined, it is equivalent to stating that, in the axis-angle representation, i^{th} link is oriented at an angle ϕ_i about an axis: $[0, \cos\theta_i, \sin\theta_i]^T$, with respect to $(i-1)^{\text{th}}$ link.

It is well know that given an axis $\boldsymbol{k} = [k_x, k_y, k_z]^T$ and an angle of rotation ϕ about the axis, $\boldsymbol{R} = \exp(\boldsymbol{K}\phi)$, where $\exp(\cdot)$ is the matrix exponential, $\boldsymbol{K}$ is the skew-symmetric matrix formed from the vector $\boldsymbol{k}$ and the corresponding exponential coordinates are $[k_x\phi, k_y\phi, k_z\phi]^T$ [11]. Hence the required exponential coordinates describing the relative motion between successive links can be obtained in terms of ϕ_i, θ_i as follows:

$$\omega_2^i = \phi_i \cos\theta_i, \tag{8}$$

$$\omega_3^i = \phi_i \sin\theta_i. \tag{9}$$

Thus we establish that for an $N-$link snake, the state vector used in this paper is of the same dimensionality as that used in [8] and the two representations are equivalent.

3) Obtaining the $SE(3)$ element: Given the state vector $\boldsymbol{x}_k$, the transformation matrix describing the pose of the most proximally located link is given by:

$$\boldsymbol{T}_0(\boldsymbol{x}_k) = \begin{pmatrix} \boldsymbol{R}_0 & \boldsymbol{p}_0 \\ \boldsymbol{0}_{1\times3} & 1 \end{pmatrix}, \tag{10}$$

where,

$$\begin{aligned} \boldsymbol{R}_0 &= \boldsymbol{I}_{3\times3} + \frac{\sin\theta}{\theta}\widehat{\boldsymbol{\omega^0}} + \frac{1-\cos\theta}{\theta^2}\widehat{\boldsymbol{\omega^0}}^2, \\ \boldsymbol{p}_0 &= \boldsymbol{V}[v_1^0, v_2^0, v_3^0]^T, \\ \boldsymbol{V} &= \boldsymbol{I}_{3\times3} + \frac{1-\cos\theta}{\theta^2}\widehat{\boldsymbol{\omega^0}} + \frac{\theta-\sin\theta}{\theta^3}\widehat{\boldsymbol{\omega^0}}^2, \\ \theta &= \text{norm}(\omega_1^0, \omega_2^0, \omega_3^0). \end{aligned} \tag{11}$$

To compute the transformation matrix $\boldsymbol{T}_i(\boldsymbol{x}_k)$ that represents the pose of i^{th} link, the following recursive process is defined:

$$\begin{aligned} \boldsymbol{T}_i(\boldsymbol{x}_k) &= \boldsymbol{T}_{i-1}\boldsymbol{T}_{i,ang}(\boldsymbol{x}_k)\boldsymbol{T}_{adv}, \\ \boldsymbol{T}_{i,ang}(\boldsymbol{x}_k) &= \begin{pmatrix} \boldsymbol{R}_i & \boldsymbol{0}_{3\times1} \\ \boldsymbol{0}_{1\times3} & 1 \end{pmatrix} \\ \boldsymbol{T}_{adv} &= \begin{pmatrix} 1 & 0 & 0 & L \\ 0 & 1 & 0 & 0 \\ 0 & 0 & 1 & 0 \\ 0 & 0 & 0 & 1 \end{pmatrix}, \end{aligned} \tag{12}$$

where L is the length of a link. The Rodrigues parameters c_2, c_3 are related to ω_2^i, ω_3^i as follows:

$$c_2 = \cos\theta \tan\frac{\phi}{2}, \tag{13}$$

$$c_3 = \sin\theta \tan\frac{\phi}{2}, \tag{14}$$

where, $\theta = \text{atan2}(\omega_3^i, \omega_2^i)$, $\phi = \sqrt{(\omega_2^i)^2 + (\omega_3^i)^2}$. The rotation matrix $\boldsymbol{R}_i$ can be obtained from c_2, c_3 as follows:

$$\boldsymbol{R}_i = \begin{pmatrix} 1-c_2^2-c_3^2 & -2c_3 & 2c_2 & 0 \\ 2c_3 & 1+c_2^2-c_3^2 & 2c_2c_3 & 0 \\ -2c_2 & 2c_2c_3 & 1-c_2^2+c_3^2 & 0 \\ 0 & 0 & 0 & 1 \end{pmatrix}. \tag{15}$$

IV. Motion and measurement model

The motion of the snake-robot has three distinct modes: advancing, retracting and steering. This section describes the motion models, $f_a(\boldsymbol{x}_k)$, $f_r(\boldsymbol{x}_k)$, $f_s(\boldsymbol{x}_k)$ respectively for the same. An electro-magnetic sensor is used to measure the position of the tip of the robot. A forward kinematic measurement model that incorporates measurement from the sensor is also described in this section.

A. Advancing and Retracting motion

When the snake is advanced by one link, the state space grows by two parameters due to addition of $\omega_2^{N-1}, \omega_3^{N-1}$. During advancement there is no relative motion between the most distal link and the link before it, therefore $\phi_{N-1} = \theta_{N-1} = 0$, which implies $\omega_2^{N-1} = \omega_3^{N-1} = 0$. Thus the motion model for advancement, $f_a(\boldsymbol{x}_k)$ remains the same as the one defined in [8]:

$$f_a(\boldsymbol{x}_k) = [\boldsymbol{x}_k^T, 0, 0]^T. \tag{16}$$

Assuming M is the length of the state vector at time-step k, the motion model for retraction is also similar to the one defined by [8]:

$$f_r(\boldsymbol{x}_k) = [\boldsymbol{I}_{(M-2\times M-2)}\boldsymbol{0}_{(M-2\times 2)}]\boldsymbol{x}_k. \tag{17}$$

The length of the state is reduced by two because the EKF would track one link less.

B. Steering motion

In [8] the relation between the differential lengths of the cables (d_1, d_2, d_3) and the orientation of the most distal link relative to the link behind it, is given. Since there exists a typographical error in the equations listed there and a derivation of the relation is not provided, the correct relation has been derived and included in this paper for the sake of completeness.

1) Steering model: The kinematic representation of two adjacent units of the snake robot is shown in Fig. 4. The units can be approximated by equilateral triangles of circumradius r whose centers are separated by a fixed distance l_c. The three cables pass through the three vertices of the equilateral triangles at the base and the top. Kinematically these can be modeled as prismatic actuators. The coordinates of the vertices of the equilateral triangle of the base link are given as:

$$\boldsymbol{b}_1 = [0, 0, r]^T, \tag{18}$$

$$\boldsymbol{b}_2 = \left[0, -\frac{\sqrt{3}r}{2}, -\frac{r}{2}\right]^T, \tag{19}$$

$$\boldsymbol{b}_3 = \left[0, \frac{\sqrt{3}r}{2}, -\frac{r}{2}\right]^T. \tag{20}$$

The coordinates of the vertices of the equilateral triangle of the top link are, given a relative rotation of $\boldsymbol{R}_i$ as defined in Eq. (15):

$$\boldsymbol{p}_k = \boldsymbol{R}_i(\boldsymbol{b}_k + [l_c, 0, 0]^T), \quad \text{for } k = 1, 2, 3. \tag{21}$$

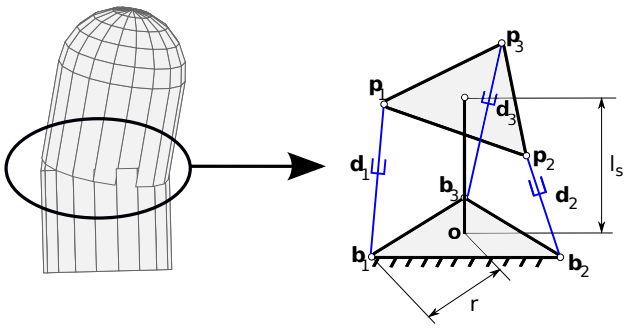

Fig. 4. Kinematic representation of two adjacent links

The length of the cables d_i, $i = 1, 2, 3$ can be obtained geometrically as the distance between $\boldsymbol{b}_i$ and $\boldsymbol{p}_i$:

$$\eta_k \triangleq (\boldsymbol{b}_k - \boldsymbol{p}_k).(\boldsymbol{b}_k - \boldsymbol{p}_k) - d_k^2 = 0, \tag{22}$$

where $k = 1, 2, 3$. The design of the robot is such that, the ratio $\frac{l_c}{r} \approx 0$. Hence, substituting this condition and simplifying yields the following constrain equations:

$$\eta_1 \triangleq 4r^2(\cos\theta_{N-1})^2 \left(\sin\frac{\phi_{N-1}}{2}\right)^2 - d_1^2 = 0 \tag{23}$$

$$\eta_2 \triangleq -r^2(-2 + \cos 2\theta_{N-1} + \sqrt{3}\sin 2\theta_{N-1}) \left(\sin\frac{\phi_{N-1}}{2}\right)^2 - d_2^2 = 0 \tag{24}$$

$$\eta_3 \triangleq r^2(2 - \cos 2\theta_{N-1} + \sqrt{3}\sin 2\theta_{N-1}) \left(\sin\frac{\phi_{N-1}}{2}\right)^2 - d_3^2 = 0. \tag{25}$$

Since there are only two unknowns, θ_{N-1}, ϕ_{N-1} and three equations, any two equations can be solved simultaneously to obtain expressions for θ_{N-1}, ϕ_{N-1}. Eliminating $\sin(\phi_{N-1}/2)^2$ from Eq. (23) and Eq. (24), one obtains:

$$\eta_4 \triangleq -2d_1^2 + 2d_2^2 + (d_1^2 + 2d_2^2)\cos 2\theta_{N-1} + \sqrt{3}d_1^2 \sin 2\theta_{N-1} = 0. \tag{26}$$

Eq. (26) is in terms of $\sin 2\theta_{N-1}$ and $\cos 2\theta_{N-1}$, by using half-tangent substitution, it can be converted to an equation wholly in terms of $\tan\theta_{N-1}$. Upon solving for $\tan\theta_{N-1}$, one obtains:

$$\tan\theta_{N-1} = \frac{\sqrt{3}d_1 + 2\sqrt{3}d_2}{3d_1},$$

$$\Rightarrow \theta_{N-1} = \arctan\left(\frac{\sqrt{3}d_1 + 2\sqrt{3}d_2}{3d_1}\right). \tag{27}$$

From Eq. (23), we obtain:

$$\phi_{N-1} = 2\left|\arcsin\left(\frac{d_1}{2r\cos\theta_{N-1}}\right)\right|. \tag{28}$$

Using Eq. (27) and Eq. (28), the change in angles from the previous time step, $\Delta\theta_{N-1}, \Delta\phi_{N-1}$ are computed and the

corresponding $\Delta\omega_2^{N-1}, \Delta\omega_3^{N-1}$ are obtained using Eq. (8). Thus the motion model for steering the snake is:

$$f_s(\boldsymbol{x}_k) = \boldsymbol{x}_k + [\mathbf{0}^T_{M-1\times 1}, \Delta\omega_2^{N-1}, \Delta\omega_3^{N-1}]^T, \qquad (29)$$

assuming M is the length of the state vector at that instant.

C. Measurement model

The tip of the highly articulated robot described in [13] is sensed by inserting an electromagnetic position sensor into one of the tool channels of the robot. The sensor used in this work is a trakSTAR™ (Ascension Technologies, Burlington, VT, USA) which has the capability to measure 6-DOF pose of the tip of the robot with respect to a world frame. Since the tracker might be removed from time to time for insertion of tools into the same channel, the roll parameter sensed, is set free. The sensor therefore observes five elements of the pose of the distal link, and the measurement model is given as:

$$h(\boldsymbol{x}_k) = [\boldsymbol{p}^T_{N-1}, \alpha_{N-1}, \beta_{N-1}]^T, \qquad (30)$$

where $\boldsymbol{p}_{N-1}$ is the position of the distal link described in terms of Cartesian coordinates and $\alpha_{N-1}, \beta_{N-1}$ are the yaw and pitch of of the distal link as measured by the sensor. The parameters $\boldsymbol{p}^T_{N-1}, \alpha_{N-1}, \beta_{N-1}$, can be obtained from $\boldsymbol{T}_{N-1}(\boldsymbol{x}_k)$:

$$\begin{aligned}
\boldsymbol{p}_{N-1} &= [\boldsymbol{T}_{N-1}(\boldsymbol{x}_k)_{1,4}, \boldsymbol{T}_{N-1}(\boldsymbol{x}_k)_{2,4}, \boldsymbol{T}_{N-1}(\boldsymbol{x}_k)_{3,4}]^T, \\
\alpha_{N-1} &= \text{atan2}(\boldsymbol{T}_{N-1}(\boldsymbol{x}_k)_{(2,1)}, \boldsymbol{T}_{N-1}(\boldsymbol{x}_k)_{(1,1)}), \\
\beta_{N-1} &= \text{atan2}(-\boldsymbol{T}_{N-1}(\boldsymbol{x}_k)_{(3,1)}, \sigma),
\end{aligned}$$

where $\sigma = \sqrt{\boldsymbol{T}_{N-1}(\boldsymbol{x}_k)^2_{(3,2)} + \boldsymbol{T}_{N-1}(\boldsymbol{x}_k)^2_{(3,3)}}$ and $\boldsymbol{T}_{N-1}(\boldsymbol{x}_k)_{i,j}$ refers to the ij^{th} term of $\boldsymbol{T}_{N-1}(\boldsymbol{x}_k)$.

D. EKF formulation

In this paper the method to estimate the state of the snake given the measurements of the position and orientation of the distal tip, is similar to the one described in [8]. The only difference is that the elements of the state vector are now in terms of exponential coordinates. It is also worth noting that we still require an advancement of atleast one link before steering it for the system to be fully observable.

V. Evaluation

Two bench-top tests were conducted to find out the effectiveness of this filtering approach. The snake robot as shown in Fig. 1, was driven using a joystick and the distal link was tracked using an electro-magnetic sensor. During the experiment time-stamped input values from the joystick as well as from the sensor were noted. After the end of the experiment, keeping the shape of the snake fixed, the sensor was pulled out of the tool-channel and a trail of data points was recorded that could be post processed and used as ground-truth.

Using the filtering approach discussed in Section. IV, the shape of the robot was estimated in both the tests. The length of each link was measured to to be 6.9 mm. The shape of the robot was also estimated using the approach described in [8] for the sake of comparison.

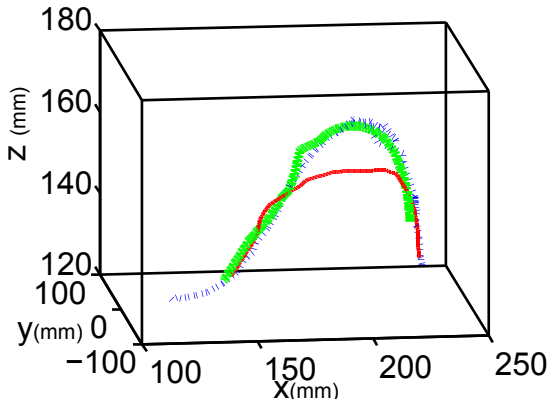

(a) Experiment 1

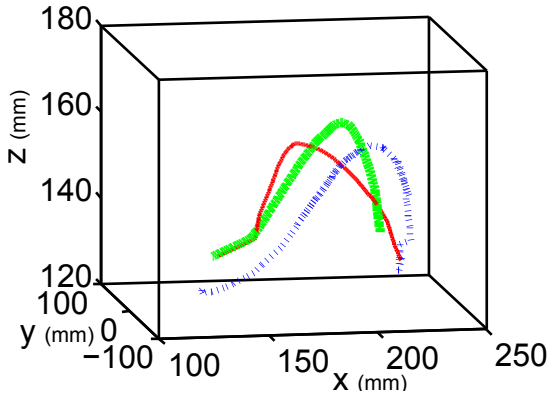

(b) Experiment 2

Fig. 5. Blue-dotted curve is the ground-truth, green-thick curve is the estimated shape using proposed approach and red-thin curve is the shape estimate using the approach described in [8]

TABLE I
Comparison between estimated shape and ground-truth

Experiment 1		
	proposed approach	approach in [8]
Standard deviation (in mm)	1.0167	3.6942
Average error (in mm)	4.7708	6.7434
Worst case error (in mm)	7.1578	13.8296
Experiment 2		
	proposed approach	approach in [8]
Standard deviation (in mm)	3.702	8.368
Average error (in mm)	16.406	18.768
Worst case error (in mm)	22.032	29.444

The average error between the estimated shape and the ground-truth in both the experiments is tabulated in Table. I. Fig. 5 shows the comparison between the ground-truth, the shape estimated by the proposed work and the shape estimated by [8]. Note how the shape estimated by the proposed approach closely approximates the ground-truth. Fig. 6 shows the variation of the error between the ground-truth and the shape estimated for various links. Notice how the proposed method has low errors throughout, which is reflected in the low standard deviation as shown in the Table. I. The improvement in the results obtained is attributed entirely

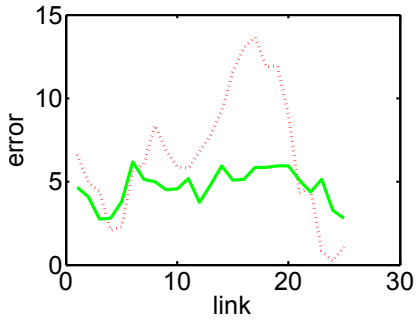

(a) Experiment 1

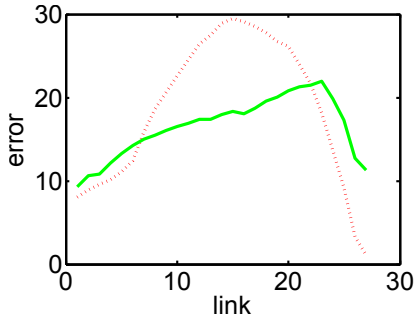

(b) Experiment 2

Fig. 6. Comparison of variation in error between estimated position and ground-truth across the links. Green line is the variation using proposed approach and red dotted line is the variation using approach described in [8]

to changing the space of the state vector to exponential coordinates.

VI. Conclusion

The goal of this work is to present an algorithm to estimate in real-time, the shape of the snake robot in an accurate manner. For medical purposes this combined with preoperative data would provide a virtual visualization of the robot inside the body relative to the organs. Our algorithm makes use of sensing the tip position using an electromagnetic sensor and motions models to predict and update the shape of the entire robot. An important contribution of this work has been describing the state at every instant, analytically in terms of the exponential coordinates and using these as state vector for the filtering to obtain more accurate estimates. Promising results have been obtained using the work described in this paper demonstrating the capability of this approach to accurately filter the configuration of the robot in real-time.

The method described above can be extended to any system as long as the motion model can be obtained in closed-form in terms of exponential coordinates. Future work would involve sensing the motor-encoder readings and using that in the measurement update step to account for uncertainties arising from inaccurate motor inputs. Also more advanced models that can capture the interaction of the robot with deformable bodies is a subject of future work.

Acknowledgment

References

[1] N. Simaan, R. Taylor, and P. Flint, "A dexterous system for laryngeal surgery," in *Robotics and Automation, 2004. Proceedings. ICRA'04. 2004 IEEE International Conference on*, vol. 1. IEEE, 2004, pp. 351–357.

[2] P. E. Dupont, J. Lock, B. Itkowitz, and E. Butler, "Design and control of concentric-tube robots," *Robotics, IEEE Transactions on*, vol. 26, no. 2, pp. 209–225, 2010.

[3] R. J. Webster and B. A. Jones, "Design and kinematic modeling of constant curvature continuum robots: A review," *The International Journal of Robotics Research*, vol. 29, no. 13, pp. 1661–1683, 2010.

[4] G. S. Chirikjian and J. W. Burdick, "A hyper-redundant manipulator," *Robotics & Automation Magazine, IEEE*, vol. 1, no. 4, pp. 22–29, 1994.

[5] K. Cleary, H. Zhang, N. Glossop, E. Levy, B. Wood, and F. Banovac, "Electromagnetic tracking for image-guided abdominal procedures: Overall system and technical issues," in *Engineering in Medicine and Biology Society, 2005. IEEE-EMBS 2005. 27th Annual International Conference of the*. IEEE, 2005, pp. 6748–6753.

[6] H. Talib, M. Styner, T. Rudolph, and G. Ballester, "Dynamic registration using ultrasound for anatomical referencing," in *Biomedical Imaging: From Nano to Macro, 2007. ISBI 2007. 4th IEEE International Symposium on*. IEEE, 2007, pp. 1164–1167.

[7] A. B. Koolwal, F. Barbagli, C. Carlson, and D. Liang, "An ultrasound-based localization algorithm for catheter ablation guidance in the left atrium," *The International Journal of Robotics Research*, vol. 29, no. 6, pp. 643–665, 2010.

[8] S. Tully, G. Kantor, M. Zenati, and H. Choset, "Shape estimation for image-guided surgery with a highly articulated snake robot," in *Intelligent Robots and Systems (IROS), 2011 IEEE/RSJ International Conference on*, 2011, pp. 1353–1358.

[9] A. Long, K. Wolfe, M. Mashner, and G. Chirikjian, "The Banana Distribution is Gaussian: A Localization Study with Exponential Coordinates," in *Proceedings of Robotics: Science and Systems*, Sydney, Australia, July 2012.

[10] A. Bry, A. Bachrach, and N. Roy, "State estimation for aggressive flight in gps-denied environments using onboard sensing," in *Robotics and Automation (ICRA), 2012 IEEE International Conference on*. IEEE, 2012, pp. 1–8.

[11] J. M. Selig, *Geometric fundamentals of robotics*, 2nd ed. New York: Springer, 1996.

[12] M. Zefran, V. Kumar, and C. B. Croke, "On the generation of smooth three-dimensional rigid body motions," *Robotics and Automation, IEEE Transactions on*, vol. 14, no. 4, pp. 576–589, 1998.

[13] A. Degani, H. Choset, A. Wolf, and M. A. Zenati, "Highly articulated robotic probe for minimally invasive surgery," in *Robotics and Automation, 2006. ICRA 2006. Proceedings 2006 IEEE International Conference on*. IEEE, 2006, pp. 4167–4172.

[14] R. M. Murray, Z. Li, and S. S. Sastry, *A Mathematical Introduction to Robotic Manipulation*. Boca Raton: CRC Press, 1994.